



HAL
open science

UHF-Dielectrophoresis Crossover Frequency as a New Marker for Discrimination of Glioblastoma Undifferentiated Cells

Rémi Manczak, Sofiane Saada, Thomas Provent, Claire Dalmay, Barbara Bessette, Gaëlle Bégaud, Serge Battu, Pierre Blondy, Marie-Odile Jauberteau, Canan Baristiran Kaynak, et al.

► To cite this version:

Rémi Manczak, Sofiane Saada, Thomas Provent, Claire Dalmay, Barbara Bessette, et al.. UHF-Dielectrophoresis Crossover Frequency as a New Marker for Discrimination of Glioblastoma Undifferentiated Cells. *IEEE Journal of Electromagnetics, RF and Microwaves in Medicine and Biology*, In press, 3 (3), pp.191-198. 10.1109/jerm.2019.2895539 . hal-02008203

HAL Id: hal-02008203

<https://hal.science/hal-02008203>

Submitted on 5 Feb 2019

HAL is a multi-disciplinary open access archive for the deposit and dissemination of scientific research documents, whether they are published or not. The documents may come from teaching and research institutions in France or abroad, or from public or private research centers.

L'archive ouverte pluridisciplinaire **HAL**, est destinée au dépôt et à la diffusion de documents scientifiques de niveau recherche, publiés ou non, émanant des établissements d'enseignement et de recherche français ou étrangers, des laboratoires publics ou privés.

UHF-Dielectrophoresis Crossover Frequency as a New Marker for Discrimination of Glioblastoma Undifferentiated Cells

Rémi Manczak , Sofiane Saada, Thomas Provent, Claire Dalmay, Barbara Bessette, Gaëlle Bégaud, Serge Battu, Pierre Blondy, Marie-Odile Jauberteau, Canan Baristiran Kaynak , Mehmet Kaynak, Cristiano Palego, Fabrice Lalloué, and Arnaud Pothier

Abstract—This paper introduces the first results of dielectric spectroscopy characterization of glioblastoma cells, measuring their crossover frequencies in the ultra-high-frequency range (above 50 MHz) by dielectrophoresis (DEP) techniques. Experiments were performed on two glioblastoma lines U87-MG and LN18 that were cultured following different conditions, in order to achieve different phenotypic profiles. We demonstrate here that the presented DEP electrokinetic method can be used to discriminate the undifferentiated from the differentiated cells. In this study, microfluidic lab-on-chip systems implemented on bipolar-complementary oxide semiconductor technology are used allowing single cell handling and analysis. Based on the characterizations of their own intracellular features, both the selected glioblastoma (GBM) cell lines cultured in distinct culture conditions have shown clear differences of DEP crossover frequency signatures compared to the differentiated cells cultured in a normal medium. These results support the concept and validate the efficiency for cell characterization in glioblastoma pathology.

Index Terms—BiCMOS chip, biological cell manipulation, glioblastoma cells, high frequency dielectrophoresis.

I. INTRODUCTION

GLIOLASTOMA (GBM) is one of the most frequent and the most aggressive tumors of the central nervous system. About 240,000 brain tumor new cases were diagnosed worldwide; the majority are GBMs with an incidence of 3–4 per 100 000 persons per year [1]. Conventional therapeutic strategy is mainly surgery, in combination with chemo- and radiotherapy

according to Stupp protocol. Despite recent advances in surgery, imaging, radiation therapies and chemotherapy, the median survival is less than 15 months [2]. This dark prognosis of GBM is primarily due to the recurrence of tumor, which is resistant to pre-cited conventional treatments [1].

Limited advances in glioblastoma treatment are closely linked to the existence of a restricted cell subpopulation also called cancer stem cells (CSCs), some very immature and undifferentiated cells, responsible for tumor cell heterogeneity [3]. However, even genetically diverse clones express undifferentiated cell markers related to cancer stem cells such as CD133 and CD44. The higher expression levels of CD133 have been correlated to poorer prognosis suggesting that this marker might play a significant role in the resistance of this type of cancer to chemotherapy and radiotherapy [4]. Other markers such as the transcription factors OCT-4, SOX2, pSTAT3, and NANOG are considered as key players in regulating transcription of glioblastoma CSCs [3]. These CSCs are a subpopulation of undifferentiated cells, which have specific biological properties similar to normal stem cells. Currently, biologists use some immunostaining approaches to characterize CSC populations, as flow cytometry, optical microscopy or protein array analysis, based on targeting a set of undifferentiated markers previously described. These markers are required to validate the stemness lineage of CSCs from the huge heterogeneous cell population. Nevertheless, CSCs subpopulation are very rare in tumors and their isolation often requires enriching them in specific culture medium. This strategy is time consuming and delays the results. Currently, the key objective is to try to get around this problem by establishing a new way to discriminate and sort undifferentiated cell populations specifically according to their biological and physical characteristics.

To optimize the diagnosis and prognosis methods, the development of different approaches and techniques based on bioelectric signals of cells have been proved to carry various helpful information on cell status [5]. Many sources of cell bioelectric signals, like sodium potassium channels and pumps in the plasma membrane, may affect chemical analytes homeostasis, cell patterning and cell-to-cell interactions with the extracellular matrix, which can be determined by exploiting the dielectric properties. Among these techniques, Dielectrophoresis (DEP) is a label-free, accurate, fast, and low-cost analysis method that

Manuscript received September 3, 2018; revised November 29, 2018; accepted January 9, 2019. Date of publication; date of current version. This work was supported by the European Union's Horizon 2020 Research and Innovation Program under Grant 737164. (*Corresponding author: Remi Manczak.*)

R. Manczak, T. Provent, C. Dalmay, P. Blondy, and A. Pothier are with XLIM-UMR 7252, University of Limoges/CNRS, Limoges 87060, France (e-mail: remi.manczak@xlim.fr; thomas.provent@xlim.fr; claire.dalmay@xlim.fr; pierre.blondy@xlim.fr; arnaud.pothier@xlim.fr).

S. Saada, B. Bessette, G. Bégaud, S. Battu, M. O. Jauberteau, and F. Lalloué are with CAPTuR-EA 3842, University of Limoges, Limoges 87025, France (e-mail: sofiane.saada@unilim.fr; barbara.bessette@unilim.fr; gaelle.begaud@unilim.fr; serge.battu@unilim.fr; m-o.jauberteau-marchan@unilim.fr; fabrice.lalloue@unilim.fr).

C. Baristiran Kaynak and M. Kaynak are with IHP, Frankfurt 15236, Germany (e-mail: baristiran@ihp-microelectronics.com; kaynak@ihp-microelectronics.com).

C. Palego is with Bangor University, Bangor LL57 1UT, U.K (e-mail: c.palego@bangor.ac.uk).

Digital Object Identifier 10.1109/JERM.2019.2895539

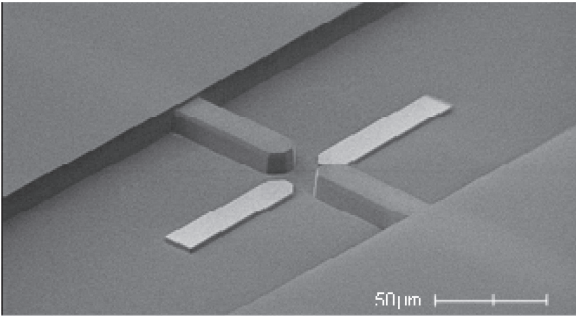


Fig. 1. Quadrupole electrodes system implemented in BiCMOS back end of line SG25H4 technology from IHP.

76 uses the principles of polarization and the motion of bio-particles
 77 in applied electric fields [6]. The efficiency of this technique has
 78 been proved in various environmental and medical fields, includ-
 79 ing polymer research, biosensors, microfluidics and diagnosis
 80 based on microfluidic biosensors [7]. In particular, manipulation
 81 of microscopic sized particles, such as trapping or cell sorting,
 82 including healthy or tumor cells suspended in microfluidic media,
 83 has been successfully demonstrated in a variety of ways
 84 using DEP methods [8]. Regarding the cellular heterogeneity in
 85 a tumor mass and different cellular subpopulations functions,
 86 we can apply the principle of DEP separation method to the
 87 cell mixture composing a tumor, especially to discriminate two
 88 cellular subpopulations with opposite differentiation properties.
 89 Based on this principle, highly represented population composed
 90 by differentiated cells are singled out from a lower undifferen-
 91 tiated subpopulation, with stemness properties. Hence, we
 92 show here a new approach to detect and characterize the undiffer-
 93 entiated cells subpopulation based on microwave dielectric
 94 spectroscopy in the Ultra High Frequency range (UHF), using
 95 DEP cell electromanipulation.

96 This approach offers unique capabilities to investigate the
 97 differences on the intracellular dielectric properties of each cell
 98 population [9]–[12] and allows screening of the intracellular
 99 biological properties and differences within the heterogeneity
 100 of a tumor.

101 II. BASICS ON CELLS ELECTROMANIPULATION BY DEP

102 When particles presenting different polarizabilities than the
 103 surrounding medium in which they are suspended are submitted
 104 to a non-uniform electric field, a DEP force is generated inducing
 105 motion of particles [13]. There are different ways to exploit this
 106 phenomenon. In the present case, a quadrupole microelectrode
 107 system [14] has been used as sensor and implemented in a
 108 microfluidic channel (see Fig. 1). For such electrode geometry,
 109 the DEP theory [7], [15], [16] shows that considering a cell as
 110 a homogeneous spherical dielectric particle, the induced DEP
 111 force can be then computed using equation (1).

$$F_{DEP} = 2\pi\epsilon_m r^3 \text{Re}[K(\omega)] \nabla |E_{rms}|^2 \quad (1)$$

$$K(\omega) = \left(\frac{\epsilon_p^* - \epsilon_m^*}{\epsilon_p^* + 2\epsilon_m^*} \right) \quad (2)$$

$$\epsilon_x^* = \epsilon_0 \epsilon_x - j \frac{\sigma_x}{\omega} \quad (3)$$

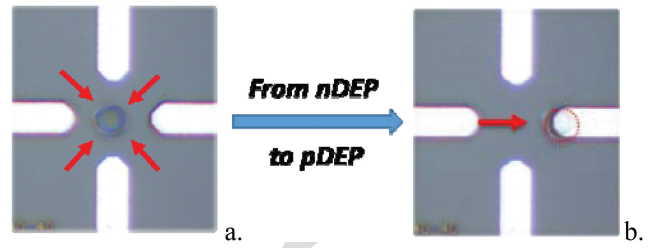


Fig. 2. DEP single cell manipulation principle. (a) Cell repulsion at system center with nDEP. (b) Cell attraction toward electrode with pDEP.

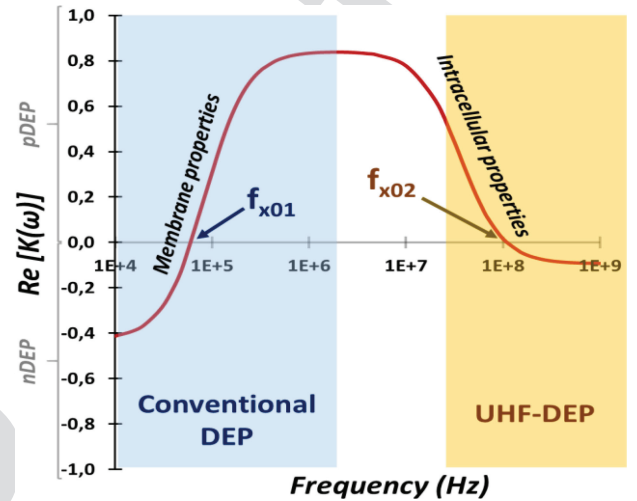


Fig. 3. Typical DEP spectral signature of cell with its two crossover frequencies f_{x01} and f_{x02} , respectively, at low and high frequency regimes.

where r is the particle radius, ω is the angular frequency of the
 applied electric field, E_{rms} is the root mean square value of this
 ∇ is the gradient operator and $\text{Re}[K(\omega)]$ the real
 part of Clausius-Mossotti factor $K(\omega)$ given by (2) in which ϵ_p^*
 and ϵ_m^* refer to the complex permittivity of the particle and the
 suspension medium, respectively. The complex permittivity ϵ_x^*
 are defined in (3), where ϵ_x and σ_x are the relative permittivity
 and conductivity either of particles or immersion medium, and
 ϵ_0 represent the electric constant ($8.854 \cdot 10^{-12} \text{ F m}^{-1}$).

By changing the frequency of the applied electric field [13],
 the polarized particles would behave in various ways depending
 on the magnitude and the sign of $\text{Re}[K(\omega)]$ which is in turn
 determined by the effective conductivity and permittivity of the
 particle and the dielectric properties of the surrounding medium.
 Therefore, particles can be individually electro-manipulated ac-
 cording to their own dielectric properties.

Actually, the generated force is repulsive when $\text{Re}[K(\omega)]$ is
 negative, meaning that the particle is repelled away from elec-
 trodes (see Fig. 2(a) negative DEP case - nDEP). Whereas when
 $\text{Re}[K(\omega)]$ is positive, the force is attractive and the particle
 moves toward the electrodes where the electric field magnitude
 is high (see Fig. 2(b) positive DEP case - pDEP). When the
 force becomes null just before the cell switches to negative to
 positive DEP (or *vice versa*), the DEP crossover frequency is
 then reached. This frequency can be thus considered as charac-
 teristic of a cell own properties and specificities and may differ
 between different cells.

139 Depending on the type of cell properties one wants to access,
 140 the choice of the DEP frequency range is important [17]–[19].
 141 If information about cell plasma membrane specificities are
 142 sought, conventional DEP frequencies (typically from 100 kHz
 143 to 5 MHz) are very suitable for cell analysis. At this low fre-
 144 quency range, the cell shape, morphology and size have strong
 145 influence on the interaction with the electric field. Conversely,
 146 Ultra High Frequencies DEP (from 50 MHz to 500 MHz) will
 147 be better to provide information about intracellular properties.
 148 Indeed, when frequency increases above several tens of MHz,
 149 the plasma membrane lets the electric field penetrate the cell
 150 and interact directly with the cell interior. As a result, the effect
 151 of DEP forces generated (i.e., attractive vs. repulsive) at high
 152 frequency regimes may be different according to the dielectric
 153 properties of the cell content. This UHF-DEP characteristic is
 154 often presented in the literature [7], [20], [21] and the crossover
 155 frequency f_{xo2} can be written by

$$f_{xo2}^2 = \frac{1}{4\pi^2} \frac{1}{\varepsilon_0^2} \frac{(\sigma_m - \sigma_p)(\sigma_p + 2\sigma_m)}{(\varepsilon_p - \varepsilon_m)(\varepsilon_p + 2\varepsilon_m)}. \quad (4)$$

156 For an aqueous solution, considering $\varepsilon_m > \varepsilon_p$ and $\sigma_p > \sigma_m$,
 157 (4) can be simplified with the approximation:

$$f_{xo2} = \frac{\sigma_p}{2\pi \varepsilon_0} \sqrt{\frac{1}{(\varepsilon_p - \varepsilon_m)(\varepsilon_p + 2\varepsilon_m)}}. \quad (5)$$

158 The value of the crossover frequency f_{xo2} in the UHF range
 159 is directly influenced by the intracellular properties of the cells,
 160 largely by its conductivity and to a lesser extent by its permit-
 161 tivity. Specifically, since undifferentiated cells exhibit different
 162 biological specificities or physiological mechanisms linked to
 163 their differentiation state for example, their crossover frequen-
 164 cies will be different from those of differentiated cells. There-
 165 fore, the analysis of their dielectrophoresis behavior under UHF
 166 frequencies seems very relevant for the targeted application.

167 III. MATERIALS AND METHODS

168 A. Cellular Culture

169 Two GBM cell lines were tested in this study, U87-MG and
 170 LN18. Both of them derived from malignant stage IV gliomas
 171 from adult patients, purchased from the American Type Culture
 172 Collection (ATCC). Two conditions were used for the analysis:
 173 (i) normal differentiation conditions in DMEM plus Glutamax
 174 medium supplemented with 10% Fetal Bovine Serum (FBS),
 175 2 mM glutamine and 100 U penicillin/0.1 mg/mL streptomycin,
 176 called NN for “Normal Normoxia Medium”, (ii) stringent con-
 177 ditions in selective DMEM/F12 medium, Define Normoxia
 178 medium (DN), supplemented with 0.6% glucose, 1.2% sodium
 179 bicarbonate, 5 mM HEPES, 9.6 μ g/mL putrescine, 10 μ g/mL
 180 ITSS, 0.063 μ g/mL progesterone, 2 μ g/mL heparin, 20 ng/mL
 181 EGF, 20 ng/mL bFGF, 1X penicillin/streptomycin and 2% B27
 182 supplement without vitamin A. Cells are maintained at 37 °C,
 183 5% CO₂ in a humidified atmosphere - 95% air incubator.

184 Actually, under stringent culture conditions, mainly only the
 185 most resistant cells with strong aggressiveness special features
 186 can survive and grow. As illustrated in Fig. 4, it is hence expected

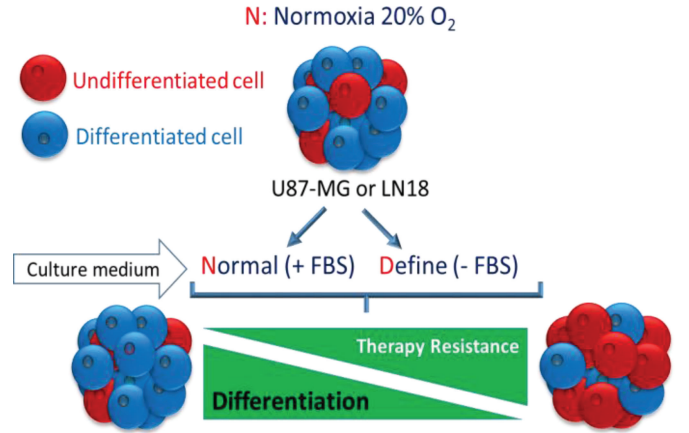


Fig. 4. Representative diagram of the two different culture conditions used for the both GBM cell lines.

to achieve a large enrichment in undifferentiated cells in DN cell
 cultures.

189 Finally, after two successive centrifuge washes, cells were
 190 suspended in an ion free osmotic medium TRIS buffer-based,
 191 composed by a water/sucrose mixture with magnesium chloride
 192 (pH: 7.4; conductivity: 26 mS/m) conventionally used for DEP
 193 experiments. The osmolarity value of this DEP medium, mea-
 194 sured with a sample of 70 μ L placed in micro-digital osmometer
 195 300-11DR (Type13) varies between 280 and 320 mOsm.

196 B. Tools and Methodology for Cell Crossover 197 Frequency Measurement

198 The main purpose of this study is to characterize GBM cell
 199 lines to identify their DEP crossover frequencies in the high fre-
 200 quency regime and establish DEP signature according to their
 201 different culture conditions (normal culture medium vs. define
 202 medium). Each cell population is introduced into the microflu-
 203 idic chip, suspended in a DEP medium, by a fluidic inlet driven
 204 by a flow controller (Fluigent MFCS) and flows in a Poly-
 205 diméthylsiloxane (PDMS) microfluidic channel implemented
 206 above dedicated sensors implemented in BiCMOS technology
 207 (see Fig. 1). The experiments were done using a 40 \times 40 μ m
 208 gap quadrupole electrodes design. This structure is based on
 209 four electrodes, set at 90°, combining a pair of thick (9 μ m)
 210 electrodes crossing the microfluidic channel with another pair
 211 of thin (0.45 μ m) electrodes implemented in the middle of the
 212 channel [14].

213 The selected 40 μ m spacing between each electrodes rep-
 214 resent a good compromise between an easy monitoring under
 215 microscope of cell motion submitted to both positive or negative
 216 DEP forces and the use of moderate RF voltage signal to bias
 217 the structure and efficiently act on cells (typically the magnitude
 218 of the applied voltage ranges between 2 and 4 V_{pp}). The same
 219 frequency adjustable DEP signal has been applied to the left and
 220 right electrodes whereas top and bottom ones were grounded.
 221 The flow is slowed down, and when a cell arrives near the center
 222 of quadrupole electrodes system, the electrodes were biased
 223 with a 500 MHz DEP signal expected to be much higher than
 224 the f_{xo2} and therefore suitable to efficiently trap cells.

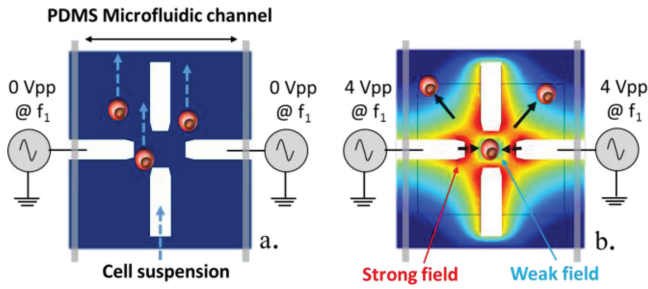


Fig. 5. Cells suspension flowing in the microfluidic system (a). Single cell nDEP trapping at 500 MHz in the center of the quadrupole electrodes related to the generated electric field (b).

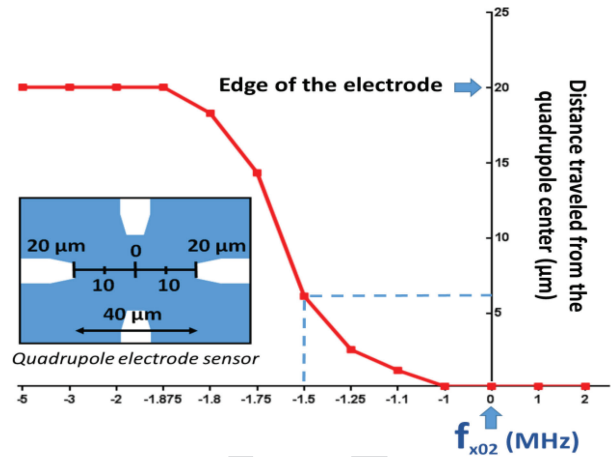


Fig. 7. Simulated cell location change from the center of the quadrupole electrodes system for different DEP signal frequency tuned around the cell crossover frequency.

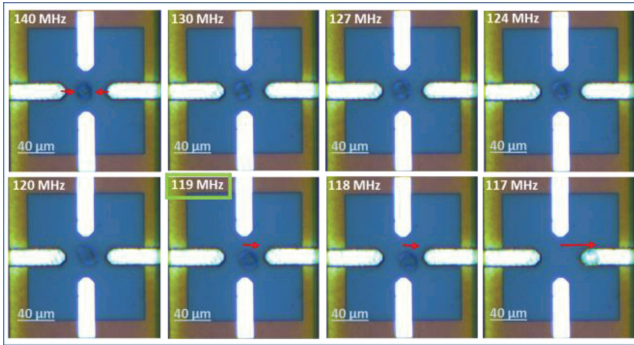


Fig. 6. Cultured in NN - Microscope imaging sequence of GBM cell crossover frequency measurement (119 MHz) by tuning the DEP signal frequency.

At 500 MHz, the cell may react in negative DEP and the generated electric field allows individually catching any single cell present near the system center. Indeed, the strong intensity field areas surrounding the center weaker field zone resulted in an electric field cage where the cell could be efficiently trapped (see Fig. 5(b)). The others surrounding cells also reacted in negative DEP and were repelled away the analysis area moving to the outside weaker intensity field zones. Then, the flow was progressively stopped and stabilized (reaching an inlet and outlet pressure equilibrium at each microchannel end). Finally, the cell was only submitted to DEP force and natural gravity. The DEP signal was first turned off for few seconds to check that the investigated cell is no longer subject to other motion forces.

Then, it was turned on again setting the signal frequency above the expected crossover frequency and the characterization could start. To determine the investigated cell crossover frequency, gradual frequencies decreases were applied on the DEP signal: first with fast 10 MHz steps and then once approaching the crossover frequency with 1 MHz ones to refine the measurement. Since the crossover frequency occurred just before the moment when the cell started to be attracted by one of lateral electrodes (switching to positive DEP behavior), a slow 1 MHz step frequency scan allowed to accurately observed this moment. Fig. 6 illustrates an example of trapping and crossover frequency characterization of a GBM cell cultured in normal medium.

Each cell was characterized hence twice or three times and finally released by increasing the inlet channel pressure to renew

medium and trap a new cell for characterization following the same approach.

This methodology of crossover frequency measurement has been supported and validated though electro-kinetic transient simulations using COMSOL software. Hence, the displacement of the trapped cell, from the center of quadrupole to the edge of the electrodes, according to the decrease of the DEP signals frequency, can be computed as presented in the graph below.

As Fig. 7 shows, the simulations predict that the generated DEP force, once applying a $4V_{pp}$ DEP signal with a frequency set to 1.5 MHz under the cell crossover frequency, should have a sufficient influence to attract and move it 6 μm away from its initial negative DEP trapping location. Actually, such displacement value matches well with the ones observed under a microscope during experiments, as illustrated on the Fig. 6 photograph taken at 118 MHz. Consequently, we can reasonably consider that using the proposed cell characterization methodology the cell crossover frequency can be measured with a 1-2 MHz accuracy.

IV. RESULTS, ANALYSIS AND CORRELATION

A. GBM Cell Lines Phenotypic Profiles

First, control experiments were carried out to confirm the enrichment of undifferentiated cell population in define medium. Comparative analysis of the gene expression (mRNA levels) of the stemness lineage was assessed in the cells cultured 6 days in normal culture medium vs. define medium (see Fig. 8). Analyzed CSCs markers (Oct-4, Sox2 and Nanog) showed an overexpression in cells cultured in define medium (in red) compared to those cultured in normal medium (in blue).

These results were completed by analyzing protein levels with flow cytometry. They showed an enhancement of undifferentiated markers expression in both U87-MG (Fig. 9(a) and (b)) and LN18 (see Fig. 9(c) and (d)) cell lines cultured in define medium compared to normal medium culture. These biological results validate the enrichment of CSC by culture in define medium.

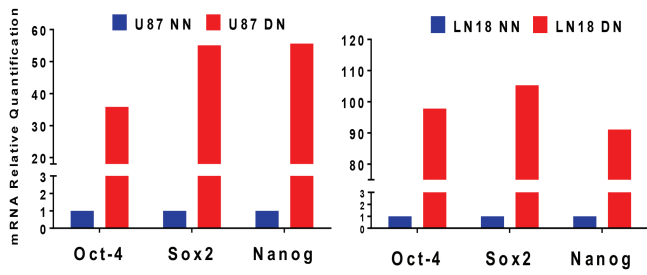


Fig. 8. Comparative analysis of gene expression of three undifferentiated markers: Oct-4, Sox2 and Nanog, in U87-MG and LN18 cell lines, cultured 6 days in normal medium (NN: blue histograms) or in define medium (DN: red histograms), measured by Real Time PCR (Polymerase Chain Reaction).

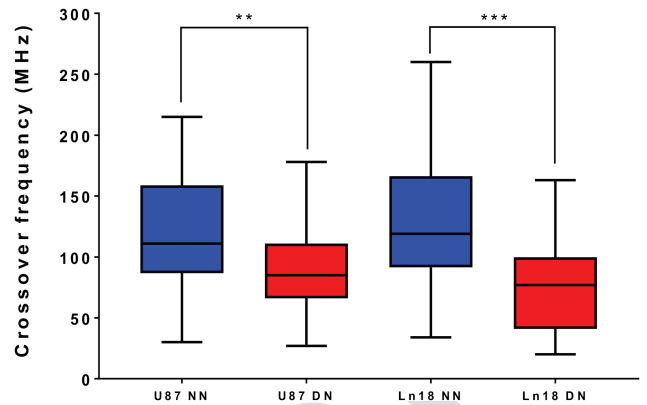
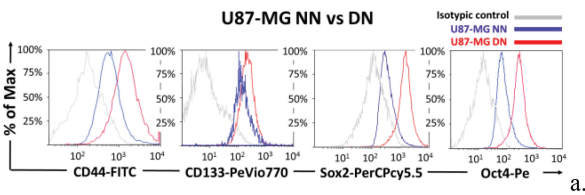


Fig. 10. Graphic box plots representation of U87-MG and LN18 cells crossover frequencies, cultured in two different conditions: normal medium (NN) and define medium (DN). The p value was determined using One-way ANOVA test. *** represents p value $< .0001$, ** represents p value $< .001$.

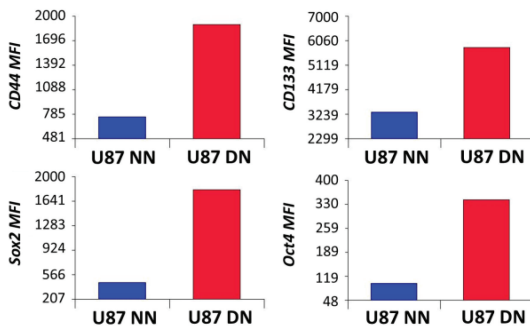
TABLE I

SUMMARY OF CROSSOVER FREQUENCY MEASUREMENTS (MHZ)

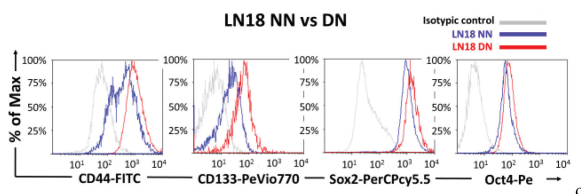
| Cell lines | Number of cells | Avg | Median | Dev Std | SEM | Min | Max |
|------------|-----------------|-----|--------|---------|------|-----|-----|
| U87 NN | 104 | 120 | 111 | 45.11 | 4.36 | 30 | 215 |
| U87 DN | 57 | 91 | 85 | 36.34 | 4.73 | 27 | 178 |
| Ln18 NN | 138 | 128 | 119 | 53.11 | 4.47 | 34 | 260 |
| Ln18 DN | 116 | 76 | 77 | 34.47 | 3.17 | 20 | 163 |



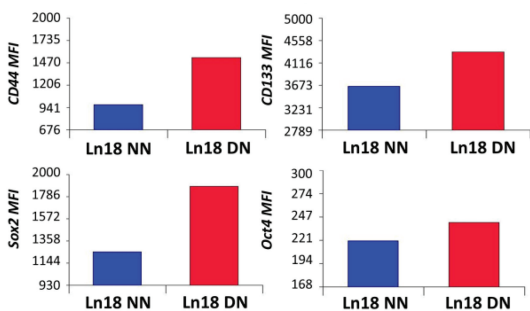
a.



b.



c.



d.

Fig. 9. Comparative analysis of the undifferentiation markers expression CD44, CD133, Oct-4, Sox2 in both U87-MG and Ln18 cell lines, cultured 6 days in normal medium (NN: blue histograms) or in define medium (DN: red histograms), analyzed by multi-parametric flow cytometry (BD Fortessa). (a) and (c) graphs represent percentage of expression and (b) and (d) histograms represent the mean fluorescent intensity (MFI) for each marker expression in U87-MG and LN18 respectively, grey graphs show the isotypes (unlabeled) negative control condition.

B. GBM Cell Crossover Frequencies

288

In order to support these results obtained at the biological level, the two GBM cell lines were characterized by establishing their UHF-DEP crossover frequencies according to their different culture conditions.

289

290

291

292

The set of crossover frequencies measured for both cell lines (U87-MG and LN18) cultured in the two different conditions (normal culture medium vs. define medium) is represented in the Fig. 10 (one should notice that the middle bar here represents the median value of the whole collected data). The considered crossover frequency corresponds to the frequency for which the trapped cell just starts to move away from the center of electrodes quadrupole. Based on statistical analysis of the results observed in the four populations, culturing cells in a define environment seems to have a real impact on the measured crossover frequencies, according to GBM intracellular characteristics changes. The set of statistics concerning the characterization of U87-MG and LN18 cells crossover frequencies is summarized in Table I, listing the average, median, standard deviation, standard error, minimum and maximum crossover frequency values for each cell population.

293

294

295

296

297

298

299

300

301

302

303

304

305

306

307

308

As shown a significant number of cells have been characterized showing statistically consolidated data. The large standard deviation, and error standard, observed for U87-MG and LN18 NN cell pool can be explained by the natural cell line

309

310

311

312

heterogeneity, including a large number of different differentiated cells but also some few undifferentiated occurrence in the pool. On the other hand, the DN cell pools may concentrate a much higher number of undifferentiated and low differentiated cells; since DN culture conditions are not favorable for differentiated cell growth.

Considering the measured crossover frequencies, these two GBM cell lines exhibit the same behavior according to the two different culture conditions. Actually, the undifferentiated enriched populations (DN) show much lower crossover frequencies than the cells cultured in normal conditions, although some crossover frequencies overlap exist between these two populations – U87-MG: Average of 120 MHz for NN vs. 91 MHz for DN – LN18: Average of 128 MHz for NN vs. 76 MHz for DN. This decrease demonstrates a significant difference (illustrated by the run ANOVA statistical analysis tests resulting in a very low p value) between these two population profiles obtained by different culture conditions. This finding proves a real difference on the intracellular dielectric characteristics of the undifferentiated cells enriched populations compared to differentiated cells, reflecting the intrinsic biological properties differences.

This difference outlines a great potential for discrimination of cell subpopulations within the whole tumor mass. Therefore such technique is highly promising to achieve discrimination and even isolation of undifferentiated cells allowing potential cell sorting of these undifferentiated subpopulations related to the CSC subpopulation.

V. CONCLUSION

We described here a novel method of cellular subpopulations' discrimination, which completes the classical biological approaches, based on the differential expression levels of a set of markers. These populations, with different cellular differentiation status, are discriminated using real time measurement on microfluidic lab-on-chip (LOC) platform implemented in CMOS technology. Both selected GBM cell lines, showed a strong correlation between the biological markers differences and the measured DEP frequency signatures according to the different culture conditions. Differences on crossover frequencies obtained for each subpopulation, showed a great discrimination potential especially for the development of a novel method to characterize Cancer Stem Cells. Thus, we confirmed the biological differences analyzed by routine methods, using DEP signatures differences, which complete the characterization of stemness properties cells. These results correlate to the biological differences at the functional level. The undifferentiated properties of CSCs are associated to intracellular changes and reflecting their high aggressiveness potential. This technic allows screening of a new cell discrimination parameter, the intracellular differences and physical properties of cells, without any labeling, without affecting cell integrity and viability. Hence, based on the UHF-DEP spectroscopy method, we detected and characterized the undifferentiated cells with unique capabilities to screen biological specificities by investigating the intracellular dielectric properties.

Finally, this method confirms a high potential of emerging lab-on-chip (LOC) platforms in the diagnosis and the treatment of glioblastoma.

REFERENCES

- [1] M. Cheray *et al.*, "Cancer stem-like cells in glioblastoma," De Vleeschouwer S1, editor. *Glioblastoma [Internet]*. Brisbane, AU: Codon, Sep. 2017, Ch. 4.
- [2] J. Chen, R. M. McKay, and L. F. Parada, "Malignant glioma: lessons from genomics, mouse models, and stem cells." *Cell*, vol. 149, no. 1, pp. 36–47, 30 Mar. 2012. doi: [10.1016/j.cell.2012.03.009](https://doi.org/10.1016/j.cell.2012.03.009).
- [3] A. Bradshaw, A. Wickremsekera, S. T. Tan, L. Peng, P. F. Davis, and T. Itintiang, "Cancer stem cell hierarchy in glioblastoma multiforme." *Front Surg*, vol. 3, p. 21, 15 Apr. 2016. doi: [10.3389/fsurg.2016.00021](https://doi.org/10.3389/fsurg.2016.00021). eCollection 2016.
- [4] F. Zeppernick, R. Ahmadi, B. Campos, C. Dictus, B. M. Helmke, N. Becker, P. Lichter, A. Unterberg, B. Radlwimmer, C. C. Herold-Mende, "Stem cell marker CD133 affects clinical outcome in glioma patients." *Clin Cancer Res.*, vol. 14, no. 1, pp. 123–9, 1 Jan. 2008. doi: [10.1158/1078-0432.CCR-07-0932](https://doi.org/10.1158/1078-0432.CCR-07-0932).
- [5] Q. Liu, C. Wu, H. Cai, N. Hu, J. Zhou, and P. Wang, "Cell-based biosensors and their application in biomedicine." *Chem. Rev.*, vol. 114, 6423–6461, 2014.
- [6] N. Abd Rahman, F. Ibrahim, and B. Yafouz, "Dielectrophoresis for biomedical sciences applications: A review," *Sensors*, vol. 17, p. 449, 2017.
- [7] R. Pethig, "Dielectrophoresis: Theory, methodology and biological applications." New York, NY, USA: Wiley, Mar. 25, 2017, doi: [10.1002/9781118671443](https://doi.org/10.1002/9781118671443).
- [8] P. R. C. Gascoyne and J. V. Vykoukal, "Dielectrophoresis-based sample handling in general-purpose programmable diagnostic instruments," in *Proc. IEEE Inst. Electr. Electron. Eng.*, vol. 92, no. 1, pp. 22–42, 1 Jan. 2004. doi: [10.1109/JPROC.2003.820535](https://doi.org/10.1109/JPROC.2003.820535).
- [9] E. Salimi, K. Braash, M. Butler, D. J. Thomson, and G. E. Bridges, "Dielectric model for Chinese hamster ovary cells obtained by dielectrophoresis cytometry," *Biomicrofluidics*, vol. 10, p. 014111, 2016. doi: [10.1063/1.4940432](https://doi.org/10.1063/1.4940432).
- [10] L. Y. Zhang *et al.*, "Discrimination of colorectal cancer cell lines using microwave biosensors," *Sensors Actuators: A. Physical*, vol. 216, no. 1, pp. 405–416, Sep. 2014.
- [11] F. Artis *et al.*, "Microwaving biological cells: intracellular analysis with microwave dielectric spectroscopy," *IEEE Microw. Mag.*, vol. 16, no. 4, pp. 87–96, May 2015.
- [12] X. Ma, X. Du, H. Li, X. Cheng, and J. C. M. Hwang, "Ultra-wideband impedance spectroscopy of a live biological cell," in *IEEE Trans. Microw. Theory Techn.*, to be published, doi: [10.1109/TMTT.2018.2851251](https://doi.org/10.1109/TMTT.2018.2851251).
- [13] H. A. Pohl, "The motion and precipitation of suspensoids in divergent electric fields," *J. Appl. Phys.*, vol. 22, 869–871, 1951.
- [14] F. Hjeij *et al.*, "UHF dielectrophoretic handling of individual biological cells using BiCMOS microfluidic RF-sensors," in *Proc. 46th Eur. Microw. Conf. (EuMC)*, London, Oct. 2016.
- [15] G. S. Fiorini and D. T. Chiu, "Disposable microfluidic devices: Fabrication, function, and application," *Bio. Techn.*, vol. 38, pp. 429–446, 2005.
- [16] L. M. Broche, F. H. Labeed, and M. P. Hughes, "Extraction of dielectric properties of multiple populations from dielectrophoretic collection spectrum data," *Phys. Med. Biol.*, vol. 50, pp. 2267–2274, 2005.
- [17] X. Du, X. Ma, H. Li, Y. Ning, X. Cheng, and J. C. M. Hwang, "Validation of Clausius-Mossotti function in single-cell dielectrophoresis," in *Proc. IEEE/MTT-S Int. Microw. Biomed. Conf.*, 2018.
- [18] K. Asami, Y. Takahashi, and S. Takashima, "Dielectric properties of mouse lymphocytes and erythrocytes," *Biochimica et Biophysica Acta*, vol. 1010, pp. 49–55, 1989.
- [19] S. Afshar, A. Fazelkhan, E. Salimi, M. Butler, D. Thomson, and G. Bridges, "Change in the dielectric response of single cells induced by nutrient deprivation over a wide frequency range," in *Proc. IEEE MTT-S Int. Microw. Symp. (IMS)*.
- [20] J. Gimsa, P. Marszalek, U. Loewe, and T. Y. Tsong, "Dielectrophoresis and electrorotation of neurospora slime and murine myeloma cells," *Biophys. J.*, vol. 60, pp. 749–760, 1991.
- [21] C. Chung, R. Pethig, S. Smith, and M. Waterfall, "Intracellular potassium under osmotic stress determines the dielectrophoresis cross-over frequency of murine myeloma cells in the MHz range," *Electrophoresis*, vol. 39, pp. 989–997, 2018.

440
441
442
443
444
445
446

Rémi Manczak received the Ph.D. degree in physics and material sciences from the University of Toulouse, Toulouse, France, in 2016. Since 2017, he has been working as a Postdoctoral Researcher Associate in the SUMCASTEC project with the University of Limoges, Limoges, France.

447
448
449
450
451
452
453
454

Sofiane Saada received the Ph.D. degree in Immunology and Oncology from the University of Limoges, France, in 2015. He was a postdoctoral associate at the University of Pittsburgh Medical Center (UPMC) (USA) (2015-2017). In 2017, he came back to University of Limoges, where he is working as a postdoctoral associate in the SUMCASTEC project.

455
456
457
458
459
460
461
462

Thomas Provent has been working toward the Ph.D. degree with the University of Limoges, France, since 2017. His research is linked directly with the SUMCASTEC project with the XLIM Research Institute on the topic of the development and characterization of a sensor to isolate and characterize cancer stem cells.

463
464
465
466
467
468
469
470
471
472
473
474
475

Claire Dalmay received the Ph.D. degree in electrical engineering from the University of Limoges, Limoges, France, in 2009. She holds a post-doctoral position with the Centre National de la Recherche Scientifique (CNRS), SATIE-BIOMIS, IFR d'Alembert, ENS Cachan, working on the development of microfluidic biochips for cell electroporation and cell handling. She is currently an assistant professor at the University of Limoges XLIM Laboratory. Her research interests are focused on microsystems for biomedical applications and additive microfabrication technologies for RF and microwave components.

476
477
478
479
480
481
482
483
484
485
486
487
488
489
490
491
492
493

Barbara Bessette received the Ph.D. degree in neuroscience and oncology from the University of Limoges, France, in 2006. She worked for one year in Paris, France, on pediatric brain tumors and the characterization of cancer stem cells in these tumors. She followed her post-doctoral experience by collaborating and working for 3 years on the GLIADYS project with IDD-Biotech (International Drug Development Biotech), specializing in monoclonal antibodies production in Lyon, France. She is currently a full-time assistant Professor at the University of Limoges in the Department of Physiology, and she leads research with the CAPTuR team. Her current research activity focuses on cancer stem cells in glioblastoma and the role of neuropeptides in their therapeutic resistance capacity. As one of the workpackages leaders in SUMCASTEC (H2020 European Project), she participates in work to determine cancer stem cell electromagnetic signature in glioblastoma and medulloblastoma.



Gaëlle Bégaud is a pharmacist who received the M.S. degree in molecular, cellular, and integrated physiopathology from the University of Toulouse, France, in 2003 and the Ph.D. degree in analytical chemistry and cellular biology from the University of Limoges, France, in 2007. In 2008, she joined Limoges University, where she is now an assistant professor in analytical chemistry and a researcher in the EA3842, CAPTuR team. Her research activity linked to the SUMCASTEC project is centered on the optimization of the use of Sedimentation Field Flow Fractionation (SdFFF) to sort Brain Cancer Stem Cells (BTSC) from complex populations such as neuroblastoma or glioblastoma cell lines. Her research interests include the implementation of new SdFFF prototypes for biological applications.

494
495
496
497
498
499
500
501
502
503
504
505
506
507
508

Serge Battu is a pharmacist who received the M.S. degree in Chemistry from the University of Toulouse, France, in 1993, and the Ph.D. degree in Cellular and Molecular Biology from the University of Limoges, France, in 1997. In 1998 he joined Limoges University, where he is now a full professor in Analytical Chemistry and instrumentation and a researcher in the EA3842 team. His research activity is centered on development of new SdFFF prototypes and to use SdFFF to sort cancer stem cells (BTSC) from complex populations such as neuroblastoma or glioblastoma cell line.

509
510
511
512
513
514
515
516
517
518
519
520
521

Pierre Blondy received the Ph.D. and Habilitation degrees from the University of Limoges, Limoges, France, in 1998 and 2003, respectively. He joined the Centre National de la Recherche Scientifique as a research engineer in 1998 and the University of Limoges in 2006, where he is currently a Professor. From 2011 to 2015, he held an Institut Universitaire de France research chair. He was a visiting researcher at the University of Michigan, Ann Arbor, USA, in 1997 and at the University of California at San Diego, La Jolla, USA, in 2006 and 2008. He founded a research group in 2003 at XLIM on innovative technologies for microwave and millimeter-wave applications, and he was involved in many research projects, funded by national and european public agencies and companies. He has been working extensively on tunable filters, RF-MEMS components, and reliability. His group is also studying the properties of phase change transition materials and their applications to microwaves. Switches, power limiters, and tunable filters have been developed using innovative materials like Vanadium Dioxide and Germanium Telluride. Dr. Blondy was an Associate Editor for the IEEE MICROWAVE AND WIRELESS COMPONENTS LETTERS in 2006. He has been a member of the IEEE International Microwave Conference Technical Program Committee since 2003, and he is also serving on the technical program of the European Microwave Conference. He is the past chair of the MTT-S Technical Committee 21 on RF-MEMS.

522
523
524
525
526
527
528
529
530
531
532
533
534
535
536
537
538
539
540
541
542
543
544
545
546

Marie-Odile Jauberteau received the Medical Doctor degree from Limoges University and the Ph.D. degree from the University of Paris VI. She has been a Medical professor of Immunology since 2000 at Limoges University, Faculty of Medicine. She is the director of the Research Team EA 3842, Control of Cell Activation, Tumor Progression and Therapeutic Resistance (CAPTuR), created in 2004. Her research is focused on oncology, especially mechanisms of cell survival and cancer stem cells.

547
548
549
550
551
552
553
554
555
556
557

558
559
560
561
562
563
564
565
566
567
568
569
570



Canan Baristiran Kaynak received the B.S degree from the Chemistry department of Istanbul Technical University and the master degree in Material Science and Engineering at Sabanci University, Istanbul, Turkey, in 2007. She received the Dr.-Ing. degree from the institute of high frequency and semiconductor system technologies from Technical University of Berlin, Germany, in 2012. Since 2008, she has held a position as scientist in the Technology Department at IHP Microelectronics. She is leading projects including heterogeneous integration of silicon-based microfluidics and microbolometer devices into BiCMOS technology.

571
572
573
574
575
576
577
578
579
580
581
582
583
584



Mehmet Kaynak received the B.S degree from the Electronics and Communication Engineering Department of Istanbul Technical University (ITU) in 2004, the M.S degree from the Microelectronic program of Sabanci University, Istanbul, Turkey in 2006, and the Ph.D. degree from Technical University of Berlin, Berlin, Germany, in 2014. He joined the technology group of IHP Microelectronics, Frankfurt (Oder), Germany, in 2008. From 2008 to 2015, he led the MEMS development at IHP. Since 2015, he has been the department head of Technology at

IHP. Dr. Kaynak is being affiliated as Adjunct Professor at Sabanci University, Turkey.

585
586
587
588
589
590
591
592
593
594
595
596
597
598



Cristiano Palego received the M.S. degree in Electrical Engineering from the University of Perugia, Italy, in 2003 and the Ph.D. degree in Microwave Engineering and Optoelectronics from the University of Limoges, France, in 2007. He was a postdoctoral associate then a research scientist at Lehigh University, Bethlehem, PA, USA, (2007–2017). In 2013, he joined Bangor University, U.K., where he is now an associate professor in smart sensors and instrumentation and a researcher in the Medical Microwave Systems group.

His research interests include micro/nanotechnology, minimally invasive animal telemetry, and biomedical technology, along with energy harvesting and RF-MEMS for reconfigurable antenna arrays.



Fabrice Lalloué received the Ph.D. degree in neurobiology and neurodevelopment from the University of Limoges, France, in 2001. He is currently Professor for the University of Limoges in the Department of Physiology and Neurosciences (Neuro-Oncology). He is also assistant director of the research team EA3842 CAPTuR (Control of cell Activation, Progression of Tumor and therapeutic Resistance) at the Faculty of Medicine. In 2000, he was visiting the Institute of Development, Aging and Cancer in Sendai, Japan. His research activities currently address

Neuro-Oncology, Glioblastoma, Brain Tumour, Initiating stem cells, adult neural stem cells, and Tumour Biomarkers. He is involved in the Scientific Pilot Committee of the Canceropole Grand Sud-Ouest consortium. He has authored or co-authored over 50 publications in research articles and conferences and holds seven patents.

599
600
601
602
603
604
605
606
607
608
609
610
611
612
613
614
615



Arnaud Pothier received the Ph.D. degree in electrical engineering from the University of Limoges, Limoges, France, in 2003. He is currently a full-time senior researcher with the XLIM research institute. His current research activity is focused on RF biosensors for label-free cell analysis. Dr. Pothier is a member of the IEEE and EuMA society, member of Technical Program Committees of IMS, EuMW, and IMBIOC Conferences, and previously served as chair of the IEEE MTT-S Technical Committee MTT-10 on Biological Effect and Medical Applications.

616
617
618
619
620
621
622
623
624
625
626
627